

Sunlight enhances calcareous deposition on cathodic stainless steel in natural seawater

M. Eashwar^{a,*}, P. Sathish Kumar^{a,b}, R. Ravishankar^b, G. Subramanian^d

^aCSIR – Central Electrochemical Research Institute, Corrosion Research Centre, Mandapam Camp - 623519, Tamil Nadu, India

^bCurrent Address: CSIR – National Institute of Oceanography, Marine Corrosion and Materials Research Division, Dona Paula, Goa - 403 004, India

^cCSIR – Central Electrochemical Research Institute, Central Instrumentation Facility, Karaikudi - 630006, Tamil Nadu, India

^dCSIR – Central Electrochemical Research Institute, Offshore Platform and Marine Electrochemistry Centre, Harbour Area, Tuticorin - 628004, Tamil Nadu, India

In replicate series of experiments in natural seawater, one in full darkness and the other in a 1:1 diurnal cycle with as little as ~ 5% of natural solar illumination, sunlight promoted calcareous deposition on cathodic stainless steel surface in a substantial manner. As exemplified by scanning electron microscopy, the deposit that formed under the natural diurnal cycle, in the presence of photosynthetic biofilms, was composed of finer calcareous crystals that provided more compact and more uniform surface coverage than the one formed in the dark. The light enhanced deposit also possessed better scale properties, as suggested by X-Ray analysis and electrochemical measurements. Sunlight enhancement of calcareous deposition looked all the more conspicuous when day and night regimes were looked at independently. These results not only bear important implications for cathodic protection in marine waters, but also provide intriguing analogy to coral reef calcification.

Keywords: stainless steel in seawater, cathodic protection, calcareous deposits, biofilms, photosynthesis, coral calcification.

*Corresponding Author: E-mail: meashwar1960@yahoo.in

Introduction

Practised throughout the world and particularly prevalent in seawater, cathodic protection (CP) utilizes the electrochemical principles of the corrosion process. Accordingly, an external current is applied to the metal to be protected, which balances the current produced from normal corrosion reactions (LaQue 1975). The application of CP generates a rise in pH at the cathode/seawater interface. The alkalinity thus generated decreases the solubility levels for calcium and magnesium dissolved in seawater, causing calcareous deposits to form on the cathode surface (Hartt et al. 1984; Johnsen 2006). The efficiency and economics of CP rely largely on the rate and chemistry of these deposits. In fact, it would be improbable to deliver the protection currents that would otherwise be required. The formation of calcareous deposits is known to be influenced by a number of factors such as hydrodynamics (Mentel et al. 1992), water temperature (Kunjapur et al. 1987; Lin and Dexter 1988; Barchiche et al. 2004), pressure (Chen et al. 2003) salinity and alkalinity (Aromaa et al. 2006; Eashwar et al. 2009) and biological fouling (Edyvean 1984; Mansfeld et al. 1990; Dexter and Lin 1992; Little and Wagner 1993; Videla et al. 1993; Eashwar et al. 2009).

An influence of sunlight on CP is just now beginning to receive attention. Benedetti et al. (2009) made the first investigation of the influence of sunlight on the CP of carbon steel in seawater. The authors reported that sunlight irradiation increased the currents required for CP, both in biologically inactivated natural seawater as well as in 3% NaCl solution. The above study, however, was conducted for a very short duration (72 hours) and under experimental conditions that were far from ambience. For instance, owing to the location of the test tanks under direct sunlight, the temperature of the seawater electrolyte in the above study fluctuated in daytime by as large as 10° C, with the possibility that other water quality parameters may have also changed. This led the above investigators to deal separately with the possible effects of heat and light. To our knowledge, there have been no other investigations on the effect of illumination on CP. Insights into the present theme of work was also provided by our recent work (Eashwar et al. 2011) in which as little as ~ 10% of full sunlight led to substantial inhibition of localized corrosion of stainless steel (SS) in natural seawater. The mechanism involved photoinhibition in addition to marked alteration of biological effects on the cathodic kinetics. This provided grounds that sunlight can also possibly influence the process of CP. Thus, the objective of the present work was to investigate what effect sunlight can have on calcareous deposition during the CP of SS under marine conditions that support the concurrent accrual of natural biofilms.

Method

Study site, materials and exposure methods

The present investigation was made in Mandapam on the southeast coast of India (9° 16' N; 79° 9' E) during February-March of the year 2011. This particular period of the year is known to have the maximal hours of sunshine at this site and a very nearly 1:1 day/night period. The mean times of sunrise and sunset during the period of this study were 06:29 h and 18:27 h respectively (Indian Standard Time). Descriptions of the site and the major water characteristics relevant for marine corrosion have been presented earlier (Eashwar et al. 2009, 2011).

Type 316 SS (UNS S31600) was the study material in this work, while carbon steel (CS) served as the sacrificial anode for effecting CP. The SS-CS combination was chosen on the basis of recent data (Eashwar et al. 2009) that a potential of ~ -0.7 V (SCE) is adequate for the CP of SS under tropical Indian conditions through the abundant formation of calcareous deposits. The metal sheets (1.1 mm thick and nominal compositions as in Table 1) were cut to 75 mm x 25 mm coupons. The coupons were pickled, polished on motor wheels with progressively finer grits and finally buffed to a very nearly 2000-grit mirror finish, degreased in acetone and rinsed in ethanol prior to use. The top of each coupon had a 5 mm drill for fastening and a 1 mm drill for copper lead connections. The metal/lead junctions were insulated by marine epoxy.

A continuous, gravity-feed and overflow set-up was employed wherein freshly sampled coastal seawater flowed from a reservoir tank (100 l) into the test tank (40 l) at a rate of about 10 l h^{-1} . An influence of illumination was investigated by employing dark and diurnal (day/night) conditions of exposure as devised in our earlier work (Eashwar et al. 2011). The dark exposures were made in a completely darkened portion of the laboratory while the diurnal exposures were set-up outdoors, underneath an opaque roof, such as to allow only diffuse sunlight to pass through. Thus, the experimental method ensured very nearly identical conditions of seawater quality in the dark and diurnal exposures, in terms of physicochemical parameters as well as the flow rate.

Coupons were fastened on to wooden frames and placed across the test tank such that the cathode to anode separation was 7.5 cm and the coupons were aligned edge-on to the flow. Couples were established using alligator clip connections as soon as the coupons were immersed in the test tanks. The SS cathodes were removed at periodic intervals over a period of 37 days. During the exposure tests, water temperature was measured using a standard mercury thermometer (0 to 50° C;

0.1°C resolution), while pH was read on a DOT-461 model digital meter. These readings were taken in the natural sea (water sampling site) as well as in the experimental tanks three times a day, around 9:00, 13:00 and 18:00 hours to ascertain the deviation in the laboratory values from the ambient. Other water quality parameters were also measured periodically following standard procedures (Strickland and Parsons 1972). Light measurements were made on a calibrated LI-COR Model LI-250A Light Meter in conjunction with Type LI-192 Quantum Sensor that permitted use in air as well as underwater. These measurements were made regularly to quantify the amount of full sunlight at the latitude of Mandapam, the diffuse light within the experimental chamber and that at the coupon location underwater.

Surface characterization

The calcareous deposits formed on the SS cathodes were examined by scanning electron microscopy (SEM) at various time periods during the seawater exposures. A simple drying procedure was followed in which the SS coupons were first gently rinsed in deionized water, cool-air-dried, and then dried in a $\text{CaCl}_2 \cdot 2\text{H}_2\text{O}$ atmosphere in a desiccator. The coupons were then observed on a Model S-3000 H, HITACHI SEM at an accelerating voltage of 20 KV. Although this procedure was not specific to biological examination of surfaces, it was very effective in capturing diatoms. It is believed that a combination of the drying technique and the siliceous nature of the diatom cells (the frustules) afforded explicit images of these photosynthetic microorganisms. An aggregate of 47 images of the diurnal coupons and 35 of the dark was analyzed, while the total field scanned and photographed was $\sim 12.6 \text{ mm}^2$. Percent cover data on calcareous deposition was obtained by importing the SEM images on to Corel PHOTO-PAINT 11 software, using gridlines to create 10^3 squares, and by measuring the filled area relative to the overall area of the pixel. The mean percent cover value was calculated by zooming in to quadruplicate images taken at 300 X. This method also permitted size measurements of fully formed calcareous crystals. Data were also obtained on the densities of diatoms occurring with the calcareous deposits, calculated as the number of cells relative to a surface area of 1 mm^2 . Diatoms were identified using keys pertinent to the study region (Santhanam et al. 1987).

Mass percentages of calcium (Ca) and magnesium (Mg) in the deposits were determined using X-Ray Fluorescence Spectroscopy (XRF, Model HORIBA XGT 2700) at the end of the 37-day exposure period, after the calcareous deposits were removed, dried and powdered on a mortar and pestle. Powder X-Ray Diffraction (XRD) patterns of the deposits were obtained on a JEOL Model JDX 8030 instrument at a step size of 0.017 ($^\circ 2\theta$) and a step time of 16 s. The scans were made in the $^\circ 2\theta$ range of 20 to 70, and the compounds were characterized using JCPDS database. Samples were

processed immediately after removal such that all surface characterization steps, including analyses, were completed within 48 h.

Electrochemical measurements

The mixed potentials of the SS-CS couples were measured on a daily basis using a high impedance voltmeter (Tektronix, Model DMM155) in conjunction with type PE-77 saturated calomel electrode (SCE) that was calibrated as previously described (Eashwar et al. 2009). The couples were disconnected at the end of the 37-day exposure periods. The potential variation trends for the disconnected SS coupons were monitored through periodic measurements of the OCP until they equilibrated. Potentiodynamic polarization tests of the SS coupons were then performed on an AUTOLAB Electrochemistry System (Model: PG STAT 30; Eco Chemie, Utrecht) at a scan rate 0.16 mV s^{-1} . A conventional three-electrode system was used with platinum as the counter electrode and SCE as reference. The electrochemical cell had a volume of 1 l, and freshly taken seawater was used as the electrolyte after $0.22 \text{ }\mu\text{m}$ membrane filtration (Millipore). The SS coupons were polarized cathodically from their equilibrium potential to -0.75 V (SCE) .

Calcareous deposition during day/night regimes

An additional experiment was conducted during February-March of 2012 in which calcareous deposition was examined during day and night times, independently, under a diurnal cycle. This study utilized experimental methods including coupon arrangements, quiescent seawater exposure and light conditions identical to those in the diurnal tests described earlier. However, the time duration to which the couples remained connected was only partial, thus setting up “day” and “night” regimes of calcareous deposition. Here, one series of the couples, designated “day”, remained connected from 30 minutes after sunrise to 30 minutes before sunset on each day of the experiment. In other words, the couples were connected 30 minutes after dawn and disconnected 30 minutes before dusk. On the other hand, the “night” samples represented an opposite of the day exposures, with a reversal of the periods of connection and disconnection everyday. Thus, these couples remained connected only in the night hours, from 30 minutes after sunset through 30 minutes before sunrise. The start of this experiment was timed in such a manner that the coupons remained coupled as soon as they were immersed in the test tanks. Thus, the day exposures commenced first, just after sunrise, while the night exposures also started the same day, but a little after sunset. This experiment lasted 14 days, at the end of which the cathode surfaces were removed and examined by SEM as previously described. A combination of 28 images each of the day and night coupons was obtained, while the total field scanned and

photographed was $\sim 6.4 \text{ mm}^2$. Percent cover and crystal size data on calcareous deposition were again computed as in the diurnal *versus* dark experiments.

Statistical analyses

One-way ANOVA was employed on Microcal ORIGIN software to evaluate the statistical significance of variance in respect of mixed potentials under diurnal and dark conditions of exposure. The above statistical test was also used to evaluate potential variation data pertaining to disconnected SS cathodes under diurnal and dark conditions. The significance of variation was calculated as statistical F and *p* values.

Results

Water characteristics and light levels

The mean ambient water temperature at the sampling site during the entire study was $29.4 \pm 1.3^\circ \text{ C}$. The mean readings in the diurnal and dark exposure tanks were $29.7 \pm 1.4^\circ \text{ C}$ and $30.3 \pm 1.1^\circ \text{ C}$ respectively. The pH of seawater ranged from 8.23 to 8.44 under all conditions. The salinity and dissolved oxygen levels during the study period varied between 33.7 and 34.8 psu and 5.6 and 6.0 mg l^{-1} , respectively. The levels of other major seawater parameters relevant for marine corrosion have been presented earlier (Eashwar et al. 2009, 2011). Light measurements showed that the average intensity of full sunlight at local noon was $1640 \pm 170 \mu\text{mol photons m}^{-2} \text{ sec}^{-1}$ during the study period. The light intensity was reduced to $\sim 10\%$ of the above level under the opaque roofed chamber, while it was further reduced to $\sim 5\%$ at the location of the coupons underwater. The amount of underwater illumination imparted on the coupons ranged from $\sim 12 \mu\text{mol photons m}^{-2} \text{ sec}^{-1}$ in the early morning and evening hours to $\sim 80 \mu\text{mol photons m}^{-2} \text{ sec}^{-1}$ at noon on a typically cloud-free day. The light level in the dark exposure area was lower than the minimum threshold of the light meter at all times ($< 0.01 \mu\text{mol photons m}^{-2} \text{ sec}^{-1}$).

Diurnal versus dark test results

The progressions of calcareous deposition on cathodic SS during seawater immersion in the diurnal and dark exposures are illustrated by SEM images in Figure 1a through 1f, all obtained at the same magnification (300 X). Under both exposure conditions, calcareous deposits after 2 days of exposure were seen to be composed of individual crystals. At this stage, the crystals that formed in the diurnal cycle appeared finer and more tightly packed, providing larger surface area coverage than those in the

dark. Percent cover data showed values of 54.5 ± 7.2 and 32.3 ± 5.6 for the diurnal and dark test conditions, respectively. Measurements of the fully formed crystals from 4 replicate frames as those in Figure 1a and 1b showed mean sizes of $21.41 \pm 2.49 \mu\text{m}$ and $30.69 \pm 3.38 \mu\text{m}$ under the diurnal and dark conditions, respectively. Calcareous deposition then passed through a stage of aggregation after 4 days, in which the crystals converged together. SEM illustrations again revealed that the deposit under the diurnal cycle was tightly filled (Figure 1c) while that in the dark was patchy and more voluminous with conspicuous hollow spaces (Figure 1d). At this time, a complete 100% calcareous deposit cover was evident under the diurnal cycle, with an unfilled area of about $37.7 \% \pm 6.8 \%$ still remaining in the dark phase. By day 7, the deposits had transformed to a structured, cauliflower-type arrangement in the diurnal phase (Figure 1e). In the dark, although the deposits transformed in shape during the corresponding exposure time, they remained more voluminous and still revealing unfilled spaces (Figure 1f). In general, the crystalline particles in the diurnal exposure showed expansion on the x-y axis, while those in the dark appeared to be stacked primarily on the z-plane.

Table 2 summarizes the taxonomic list and the densities of diatoms associated with calcareous deposits on the diurnal SS samples after a 2 and 7 days of exposure to natural seawater. In quantitative terms, *Amphora* spp., *Navicula* spp. and *Bacillaria paradoxa* showed relatively higher densities over the other diatoms at 2 d, while *Amphora* spp. exclusively dominated the community at 7 d exposure. The deposit in the dark was devoid of diatoms at any time.

XRD patterns for the calcareous deposits (Figure 2) revealed mostly aragonite form of CaCO_3 (designated “A”) under both conditions of exposure, although some departures were readily apparent. The aragonite peaks in the diurnal exposure appeared stronger in intensity; also, there were 5 additional aragonite peaks here than in the dark. Furthermore, the 3 calcite peaks noted in the dark (designated “C”) were altogether missing in the diurnal exposure. XRF data in Figure 3 shows that the deposit in the diurnal cycle was almost exclusively Ca (with only 0.4% Mg), while that in the dark had much higher content of Mg (6.1%).

The mixed potentials of the SS-CS couples depicted in Figure 4a are the means of 5 SS coupons for each category, showing slightly more negative values for the diurnal couples than those for the dark couples at any given time. The difference became particularly obvious during the second half of the exposure period, being consistently ~ 10 mV. Although this difference would, at a first glance, appear rather small, the statistical significance of the variance was enormous ($F = 38.82$; $p = 2.56 \times 10^{-8}$). Disconnection of the SS-CS couples led to potential variation patterns as shown in Figure 4b, where the data are again the means of 5 coupons for each category. The potentials in the dark dropped down

to ~ -0.1 V (SCE) within an hour, while those in the diurnal cycle did so more slowly and remained more negative, at values ~ -0.25 V (SCE), over several hours. Again, the statistical significance of the variation between the diurnal and dark data was remarkably very high ($F = 75.44$; $p = 3.19 \times 10^{-8}$). Potentiodynamic polarization curves obtained on the above coupons are illustrated in Figure 5. The scans show markedly smaller current densities in the diurnal cycle than those in the dark, particularly down to ~ -0.5 V (SCE). The variation in current density was very nearly two orders of magnitude at -0.2 V (SCE) and about one order of magnitude at -0.5 V (SCE), as it gradually narrowed down to a certain extent at the more negative potentials.

Day versus night test results

The images in Figure 6(a)-6(d) illustrate the influence of day/night regimes on calcareous deposition and associated diatom settlements after 14 days of exposure to natural seawater. Consistent with the results for diurnal *versus* dark phases, day-time deposits (Figures 6(a) and 6(c)) appeared finer and more tightly packed than those formed at night (Figures 6(b) and 6(d)). Thus, day-time deposits provided 69.8 ± 7.9 % coverage of the cathodic SS surface, while night-time deposits were substantially lower in percent cover (14.7 ± 4.4). The mean sizes of fully formed calcareous crystals were 11.86 ± 1.81 μm in the day and 21.45 ± 2.44 μm at night, respectively.

By virtue of the outdoor exposure and a diurnal cycle employed in this experiment, diatoms were associated with calcareous deposition under day as well as night phases. Table 3 summarizes the taxonomic list and the densities of diatoms after 14 days of exposure under day and night regimes of calcareous deposition. The microfloral composition remained almost identical to that in the diurnal exposure (Table 2), barring the exclusion of the centric diatom *Coscinodiscus* sp. and the addition of the pennate diatom, *Achnanthes longipes*. The data in Table 3 reveal that the overall diatom density associated with night-time calcareous deposits was three-fold higher than that associated with day-time deposits.

Discussion

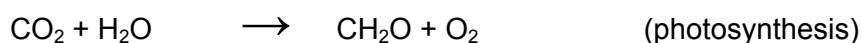
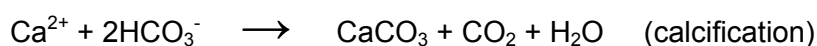
It becomes very clear from this study that sunlight has a promoting effect on the process of calcareous deposition on SS surfaces in seawater. As exemplified by SEM, the calcareous deposit under a natural diurnal cycle was composed of finer calcareous crystals that provided more compact and more uniform surface coverage than the one formed in the dark (Figure 1). Corresponding variations of deposit morphology were also evident when day- and night-time patterns were independently inspected (Figure

6). The deposit that formed in the presence of light also possessed better scale properties in terms of the chemical composition (Figures 2 and 3). In general, aragonite is acknowledged to be more protective than calcite (Liu et al. 2011). Also, Ca:Mg ratio has historically been considered as a reasonable measure of the scale quality, with the lower amount of Mg in the deposit generally reflecting better protectiveness (Hartt et al. 1984; Okstad et al. 2007). It is possible that the higher amount of Mg in the deposit formed in the dark was calcite related, as Mg is known to adsorb on the surface of calcites, also causing an increase in surface roughness and distortion of crystals (Chen et al. 2005). It is believed that the potential variation trends for the SS cathodes upon disconnection (Figure 4b) reflect the potency of cathodic polarization during the coupling and, consequently, the stability of the formed calcareous deposit. Thus, the propensity of the disconnected SS samples to sustain a more negative potential, which was stronger for the diurnal than for the dark, is believed to be an indicator of scale quality. Additionally, the cathodic polarization data (Figure 5) can be taken to mean that the current density requirements for cathodically protecting SS in seawater should be considerably lowered by sunlight. The overall results from this work are discussed below from perspectives of possible mechanisms of sunlight-enhanced calcareous deposition and the implications of the present data.

Two possible scenarios come into picture in explanation of the observed results, the first involving the semiconducting property of the surface passive film on SS. It has been well established that illumination can enhance the passivity of SS in its open-circuit and lead to substantial reduction of localized corrosion initiation and propagation in neutral chloride media (MacDonald and Heaney 2000; Moussa and Hocking 2001; Fujimoto and Tsuchiya 2007). The phenomenon, known as photoinhibition, has lately been shown to occur under practical seawater situations also, through significant alteration of both anodic and cathodic processes on SS (Eashwar et al. 2011). The passive film that forms on SS surface in seawater is generally an n-type, where the potential shift from illumination would be in the cathodic direction (Faimali et al. 2008; Eashwar et al. 2011). The consistently more negative mixed potentials for diurnal samples over those in the dark phase (Figure 4(a)), which was statistically significant on a very high note, can be deemed to reflect a photoelectrochemical effect. For an n-type alloy such as UNS S31600 in the present work, illumination can be envisioned to produce a change in the Fermi level due to the promotion of electrons to the conduction band (MacDonald 1999). Consequently, it is possible that sunlight transformed the passive film to one that was more conductive, thus enhancing the cathodic reaction and hence calcareous deposition.

The second possibility is biologically enhanced calcification, through the photosynthetic activity of microorganisms accrued on to cathodic SS surfaces concomitantly with the calcareous deposits. The biologically assisted phenomenon proposed here is analogous to coral reef development (eg Gattuso et

al. 1999; Cohen and McConnaughey 2003) where sunlight is known to promote aragonite calcification through an enhancement of the photosynthesis carried out by symbiotic organisms known as the zooxanthellae. Indeed, coral calcification is known to occur 3 to 5 times faster in day-time than at night (Moya et al. 2006). It is generally accepted that calcification and photosynthesis proceed according to the following equations (Gattuso et al. 1999):



where the production of CO_2 within the skeletal material is removed by photosynthesis. It is also acknowledged (Gattuso et al. 1999) that calcification may, in turn, stimulate photosynthesis by supplying CO_2 . In the present work, the general presence of photosynthetic diatoms in association with the deposits (Table 2) provides adequate inference that the biofilm in the diurnal phase was photosynthetically active while that in the dark was almost certainly not. Although more numbers of diatoms were seen associated with the night-time deposit rather than with the light-enhanced day-time deposit (Table 3), contrary to what one might expect, it must be taken into account that photosynthetic activity and the promotion of calcification may be controlled by the physiology of the algae rather than algal cell numbers (eg Abramovitch-Gottlib et al. 2005). Also, calcium (Geesey et al. 2000) and alkalinity (Nandakumar et al. 2003) can favour the physiology of certain species of diatoms. Indeed, the dominant presence of *Amphora* spp. on cathodic surfaces in this work (Tables 2 and 3) could possibly be attributed to the abovementioned effects. It must additionally be considered that the surface preparation procedure adopted in this work compromised biological examination of surfaces to some extent. The simple drying procedure was preferred over conventional fixing and dehydration steps in order to retain the configuration of the deposits, which otherwise appeared deformed (Eashwar et al. 2009). Thus, the SEM technique employed in this work disregarded other microorganisms such as bacteria and cyanobacteria that also contribute to photosynthesis. The significance of the biological mechanism on light enhanced calcareous deposition in the context of cathodic surfaces should form a very interesting pursuit.

Regardless of the major mechanism, the present results suggest a substantial benefit from sunlight. Although most studies of calcareous deposition and improvements in the application of marine CP have concentrated on CS, the increasing number of offshore structures for oil and gas production and the introduction of more sophisticated alloys have made studies of CP equally important for SS

(Kim and Hartt 2006). The difficulty in obtaining a good calcareous deposit in deep ocean waters, accompanied by increased current demand, is particularly well known for both CS and SS (Kim and Hartt 2006; Johnsen 2009). This has been attributed mainly to the lower water temperature. A possible influence of the darkness characteristic of these waters now transpires from this work.

Besides raising the inquiry of the predominant mechanism of sunlight enhanced calcareous deposition, the present work also provides strong impetus for future works in at least three directions. The first is an examination of the extent to which illumination along a vertical profile can influence calcareous deposition, with CS as well as SS as cathodes, in water columns ranging from shallow coastal areas to the deep ocean. The second would be to explore the prospect of applying illumination as an innovative approach to augment calcareous deposition and related criteria involved in marine CP. Thirdly, the application of electrochemistry is becoming popular with induced mineral accretion technique used in coral restoration processes (Hilbertz and Goreau 1996; Sabater and Yap 2004; Benedetti et al. 2011). This method uses cathodic currents for enriching aragonite on metallic substrata that apparently stimulates larval settlement and also promotes calcification of transplanted coral nubbins. Thus, it is believed that the revelations made in the present work would be highly relevant, interesting and advantageous to investigators in the above subject area as well.

Conclusions

- A strong influence of sunlight was noted in the present study in which light levels as low as ~ 5% of full solar illumination promoted calcareous deposition during the cathodic protection of UNS 31600 in natural seawater.
- The light enhanced calcareous deposit possessed improved scale properties over the one formed in the dark, as evaluated by SEM (morphology), XRF (Ca; Mg ratio) and potentiodynamic polarization (current densities).
- Sunlight enhancement of calcareous deposition was also marked when day and night phases were independently examined in a diurnal exposure. The phenomenon of light enhanced calcareous deposition appears strikingly similar to coral reef calcification.
- The present work has strong implications for marine cathodic protection as well as electrochemical stimulation of coral restoration.

Acknowledgements

The authors are grateful to Dr. V. Yegnaraman, former Director, and Dr. Vijayamohan K. Pillai, the present Director, CSIR – Central Electrochemical Research Institute, Karaikudi, India for their encouragement and support. Special appreciations go to C. Cyril Stephen, K. Krishnamoorthy, T. Jeyaram, L. Subbiah and M. John Peter for their valuable technical support at the Mandapam laboratory.

References

Abramovitch-Gottlib L, Dahan D, Golan Y, Vago R. 2005. Effect of light regimes on the microstructure of the reef-building coral *Fungia simplex*. *Mat Sci Eng C* 25:81-85.

Aromaa J, Pehkonen A, Forsén O. 2006. Cathodic protection of ships in brackish waters. *J Solid State Electrochem* 10:681-688.

Barchiche C, Deslouis C, Gil O, Efait P, Tribollet B. 2003. Characterisation of calcareous deposits in artificial seawater by impedance techniques. *Electrochim Acta* 49:2833-2839.

Benedetti A, Magagnin L, Passaretti F, Chelossi E, Faimali M, Montesperelli G. 2009. Cathodic protection of carbon steel in natural seawater: effect of sunlight radiation. *Electrochim Acta* 54:6472-6478.

Chen S, Hartt WH, Wolfson S. 2003. Deep water cathodic protection. *Corrosion* 59:721-732.

Chen T, Neville A, Yuan M. 2005. Assessing the effect of Mg^{2+} on $CaCO_3$ scale formation-bulk precipitation and surface deposition. *J Crystal Growth* 275:1341-1347.

Cohen AL, McConnaughey TA. 2003. Geochemical perspectives on coral mineralization. *Rev Mineral Geochem* 54:151-187.

Dexter SC, Lin SH. 1992. Effect of marine bacteria on calcareous deposition. *Int Biodeterior Biodegrad* 29:231-249.

Eashwar M, Subramanian G, Palanichamy S, Rajagopal G, Madhu S, Kamaraj P 2009. Cathodic behaviour of stainless steel in coastal Indian seawater: calcareous deposits overwhelm biofilms. *Biofouling* 25:191-201.

Eashwar M, Subramanian G, Palanichamy S, Rajagopal G. 2011. The influence of sunlight on the localized corrosion of UNS S31600 in natural seawater. *Biofouling* 27:837-849.

Edyvean RGJ. 1984. Interactions between microfouling and the calcareous deposit formed on cathodically protected steel in seawater. *Proc. 6th international congress on marine corrosion and fouling*. Athens, Greece. p. 469-483.

- Faimali M, Chelossi E, Garaventa, F, Corrà C, Greco, G, Mollica A. 2008. Evolution of oxygen reduction current and biofilm on stainless steels cathodically polarized in natural aerated seawater. *Electrochim Acta* 54:148-153.
- Fujimoto S, Tsuchiya H. 2007. Semiconductor properties and protective role of passive films of iron base alloys. *Corros Sci* 49:195-202.
- Gattuso JP, Allemand D, Frankignoulle M. 1999. Photosynthesis and calcification at cellular, organismal and community levels in coral reefs: a review on interactions and control by the carbonate chemistry. *Am Zool* 39:160-183.
- Geesey GG, Wigglesworth-Cooksey B, Cooksey KE. 2000. Influence of calcium and other cations on surface adhesion of bacteria and diatoms: a review. *Biofouling* 15:195-205.
- Hartt WH, Culberson CH, Smith SW. 1984. Calcareous deposits on metal surfaces in seawater: a critical review. *Corrosion* 40:609-618.
- Hilbertz WH, Goreau TJ, 1996. Method of enhancing the growth of aquatic organisms, and structures created thereby. US Patent no. 5,543, 034.
- Johnsen R. 2006. Cathodic protection. Trondheim, Norway: NTNU Report, October 2006, 27 p.
- Johnsen R. 2009. Cathodic protection in cold seawater: current density requirements. *Corrosion/2009*, paper no. 09521, Houston, TX: NACE International.
- Kim K, Hartt WH. 2006. Characteristics of cathodic protection and calcareous deposits for type 316L stainless steel in simulated deep sea conditions. *Corrosion/2006*, paper no. 06104, Houston, TX: NACE International.
- Kunjapur S, Hartt WH, Smith SW. 1987. The influence of temperature on calcareous deposition. *Corrosion* 43:674-679.
- LaQue FL, editor. 1975. *Marine corrosion: causes and prevention*. New York, London, Sydney and Toronto: John Wiley and Sons. 332 pp.
- Lin SH, Dexter SC. 1988. Effect of temperature and magnesium ions on calcareous deposition. *Corrosion* 44:615-622.
- Little B, Wagner P. 1993. The interrelationship between marine biofouling and cathodic protection. *Mater Perform* 32:16-20.
- Liu FG, Wu SR, Lu CS. 2011. Characterisation of calcareous deposits on freely corroding low carbon steel in artificial sea water. *Corros Eng Sci Technol* 46:611-617.
- MacDonald DD. 1999. Passivity: the key to our metal-based civilization. *Pure Appl Chem* 71:951-978.

MacDonald DD, Heaney DF. 2000. Effect of variable intensity ultraviolet radiation on passivity breakdown of AISI type 304 stainless steel. *Corros Sci* 42:1779-1799.

Mansfeld F, Tsai R, Shih H, Little B, Ray R, Wagner P. 1990. Results of exposure of stainless steels and titanium to natural seawater. *Corrosion/90*. Houston, TX: NACE International. paper no. 109.

Mantel KE, Hartt WH, Chen TY. 1992. Substrate, surface finish and flow rate influences on calcareous deposit structure. *Corrosion* 48:489-499.

Moussa SO, Hocking G. 2001. The photo-inhibition of localized corrosion of 304 stainless steel in sodium chloride environment. *Corros Sci* 43:2037-2047.

Moya A, Tambutté S, Tambutté E, Zoccola D, Caminiti N, Allemand D. 2006. Study of calcification during a daily cycle of the coral *Stylophora pistillata*: implications for 'light-enhanced calcification' *J Exp Mar Biol Ecol* 209:3413-3419.

Nandakumar K, Matsunaga H, Takagi M. 2003. Microfouling studies on experimental test blocks of steel-making slag and concrete exposed to seawater off Chiba, Japan. *Biofouling* 19:257-267.

Okstad T, Rannestad Ø, Johnsen R, Nisancioglu K. 2007. Significance of hydrogen evolution during cathodic protection of carbon steel in seawater.

Corrosion 63:857-865.

Sabater MG, Yap HT. 2004. Long-term effects of induced mineral accretion on growth, survival and corallite properties of *Porites cylindrica* Dana. *J Exp Mar Biol Ecol* 311:355-374.

Santhanam R, Ramanathan N, Venkataramanujam K, Jagatheesan G. 1987. Phytoplankton of the Indian seas. New Delhi (India): Daya Publishing House. 134 pp.

Strickland JDH, Parsons TR, 1978. A practical handbook of seawater analysis. Ottawa: Fisheries Research Board of Canada. 310 pp.

Videla HA, Gomez de Saravia SG, de Mele M. 1993. Early stages of bacterial biofilm and cathodic protection interactions in marine environments. *Proc 12th int corrosion congress*. Houston, TX: NACE International. p. 3687-3695.

Table 1. Nominal compositions of the alloys used in the present work.

Alloy name	Cr	Ni	Mo	Fe	C	Mn	P	S
	316 SS	17.0	7.0	2.1	Bal.	0.07	---	---
Carbon steel	---	---	---	Bal.	0.1	0.46	0.07	0.03

Table 2. Taxonomic list and densities of diatoms associated with calcareous deposits on cathodic SS samples under the diurnal cycle after 2 and 7 days of exposure to natural seawater.

Diatom species	Density, cells mm ²	
	2-d exposure	7-d exposure
<i>Amphora</i> spp.	32	588
<i>Bacillaria paradoxa</i>	20	0
<i>Coscinodiscus</i> sp.	4	0
<i>Diploneis robustus</i>	8	0
<i>Navicula henneydii</i>	16	6
<i>Navicula longa</i>	14	8
<i>Nitzschia sigma</i>	6	0
<i>Pleurosigma</i> sp.	6	0
<i>Thalassiothrix</i> sp.	8	0
Total cells	114	602

Table 3. Taxonomic list and densities of diatoms on cathodic SS samples after 14 days of exposure to natural seawater under day and night regimes of calcareous deposition

Diatom species	Density, cells mm ²	
	Day	Night
<i>Achnanthes longipes</i>	46	178
<i>Amphora</i> spp.	120	340
<i>Bacillaria paradoxa</i>	40	122
<i>Diploneis robustus</i>	22	66
<i>Navicula henneydii</i>	60	148
<i>Navicula longa</i>	18	52
<i>Nitzschia sigma</i>	6	68
<i>Pleurosigma</i> sp.	2	24
<i>Thalassiothrix</i> sp.	28	10
Total cells	342	1008

Figure 1

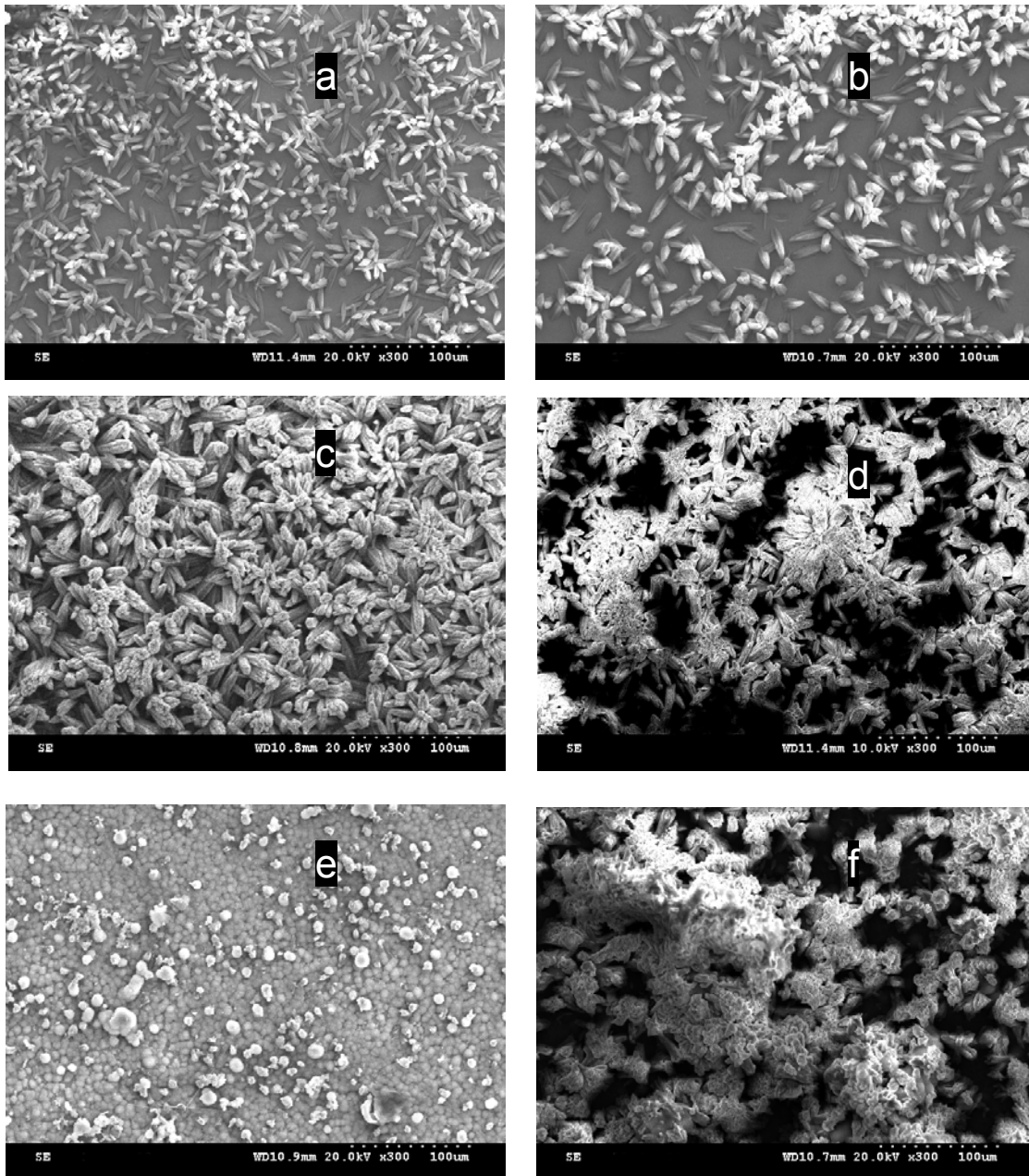


Figure 2

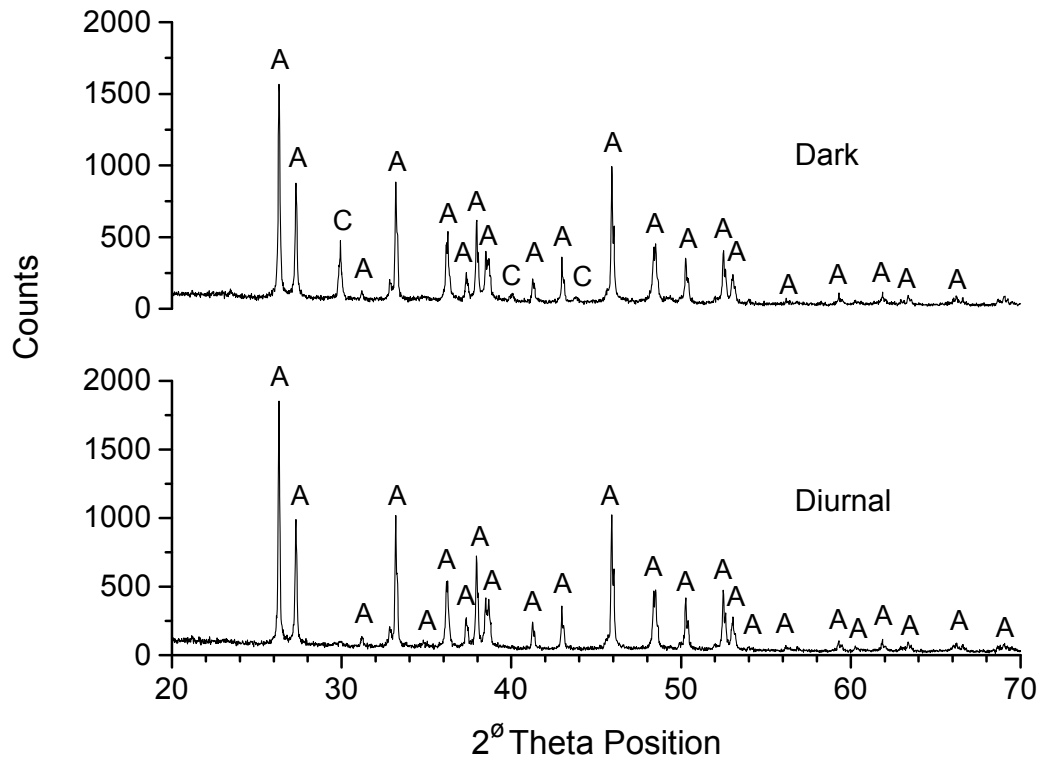


Figure 3

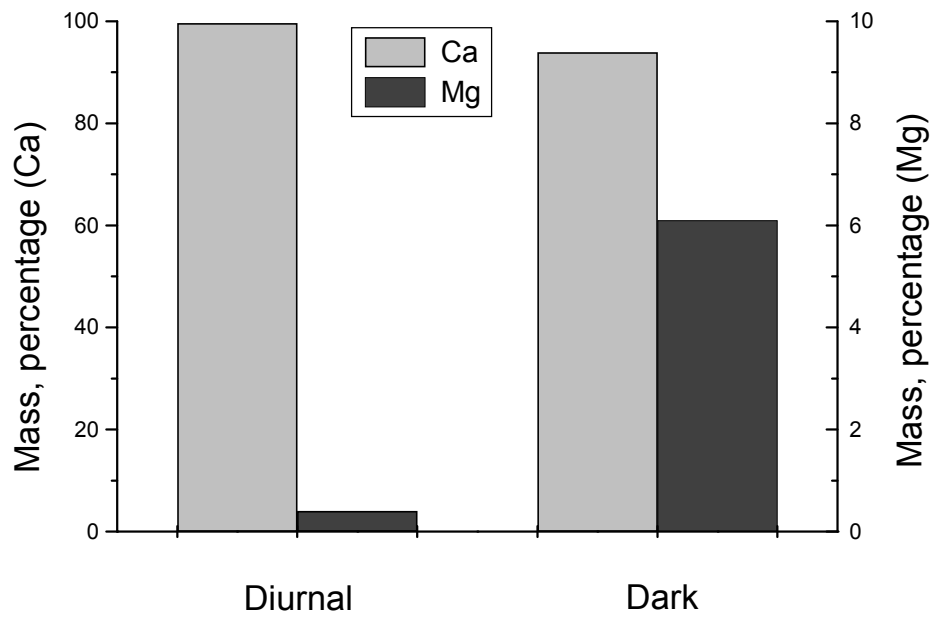


Figure 4

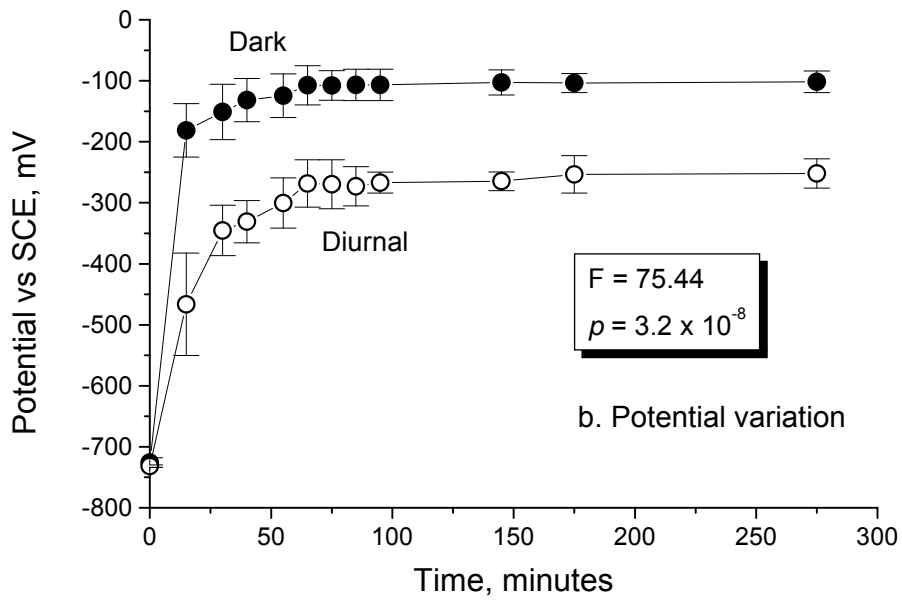
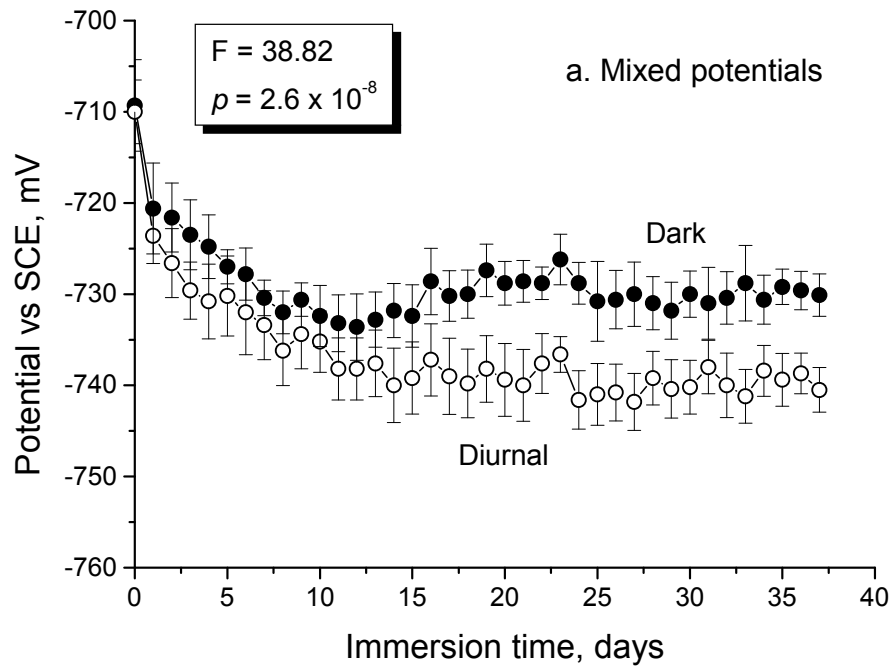


Figure 5

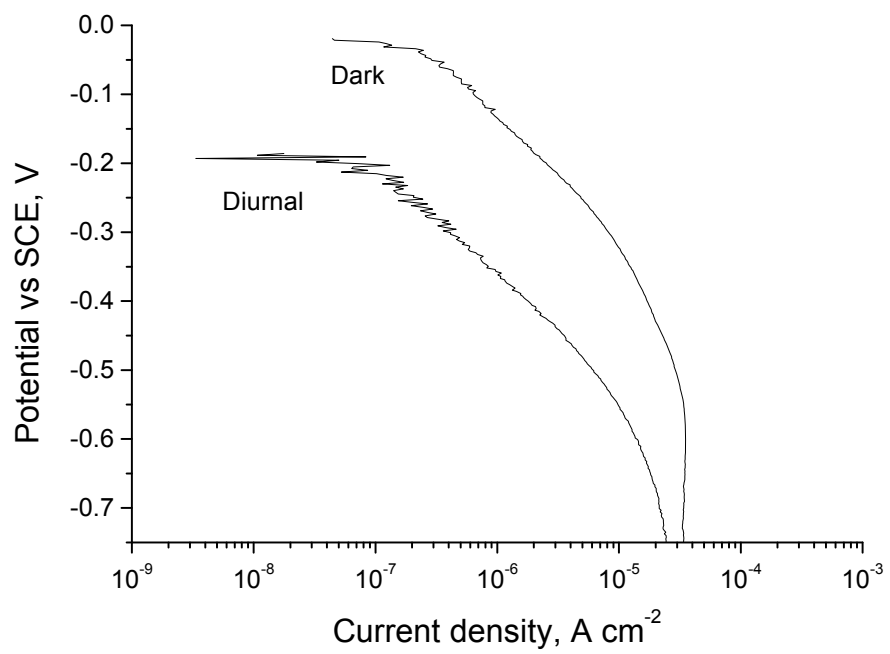


Figure 6

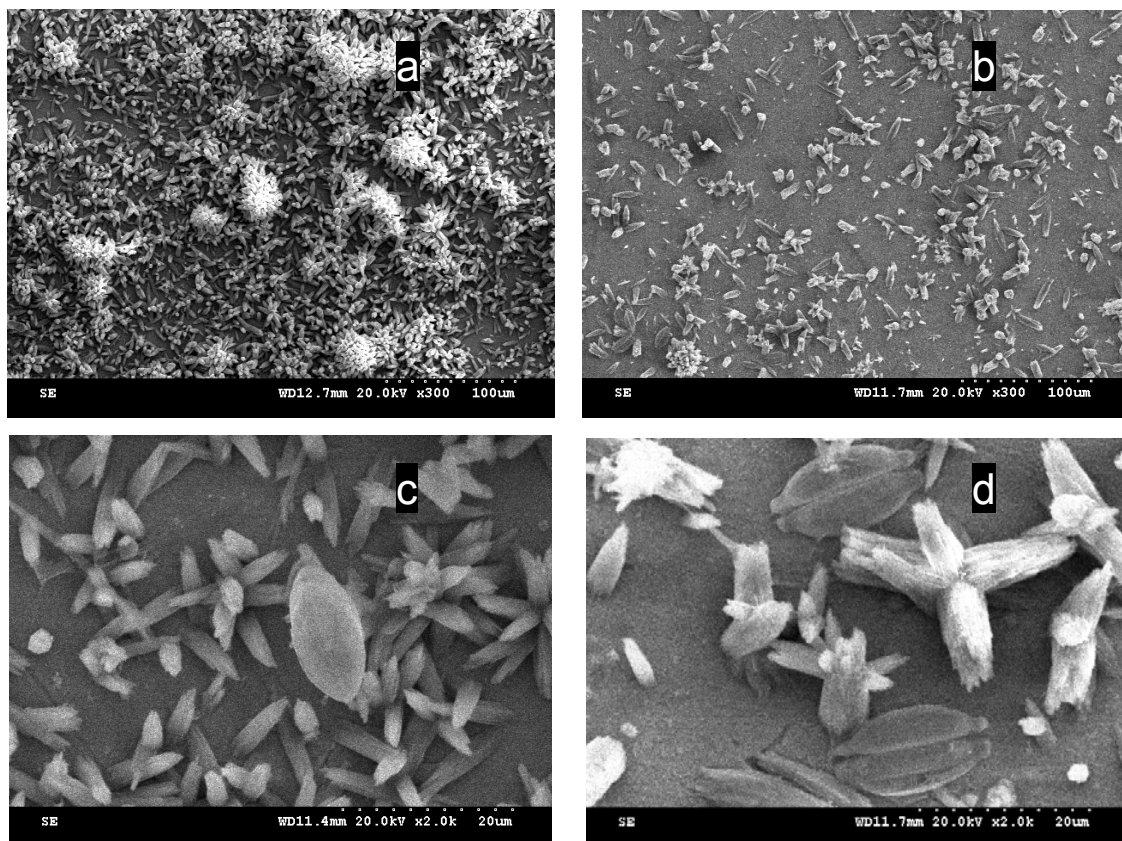
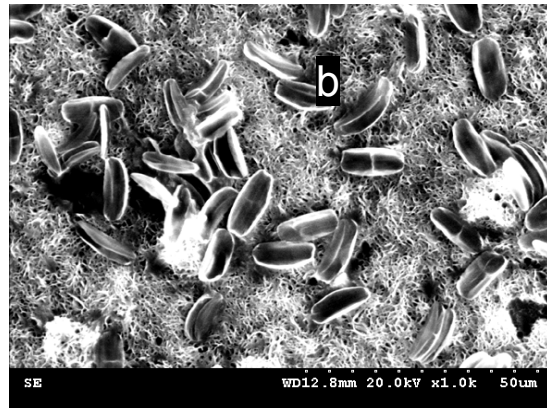
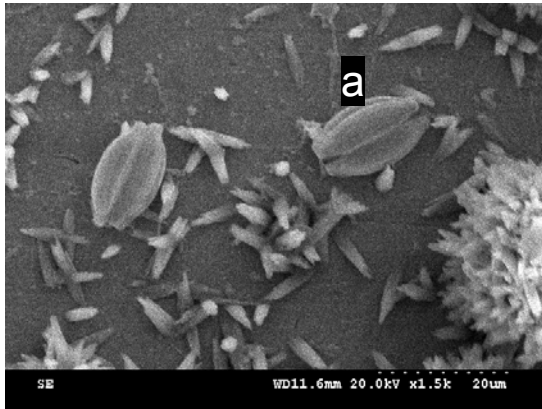


Figure 7



Captions for Figures

Figure 1. Morphology of calcareous deposits formed on cathodic SS surfaces after 2 (a, b), 4 (c, d) and 7 (e, f) days of exposure to natural seawater. The images (a), (c) and (e) show deposits under diurnal condition, while (b), (d) and (f) are corresponding images for dark, all at 300 X.

Figure 2. XRD patterns for calcareous deposits formed on cathodic SS surfaces after natural seawater exposure for 37 days under diurnal and dark conditions. “A” denotes aragonite phases, while “C” stands for calcite.

Figure 3. XRF data showing Ca and Mg ratios for calcareous deposits formed on cathodic SS surfaces after natural seawater exposure for 37 days under diurnal and dark conditions.

Figure 4. Mixed potentials for the SS-CS couples with time during the natural seawater exposure exposures under diurnal and dark conditions (a) and potential variation trends with time for the SS cathodes after the disconnection of the couples (b).

Figure 5. Potentiodynamic polarization scans for the SS cathodes exposed to natural seawater under diurnal and dark conditions, after 48 hours of disconnection.

Figure 6. Morphology of calcareous deposits formed on cathodic SS surfaces after 14 days of exposure to natural seawater under day-night cycles. The images (a) and (c) show deposits formed in day-time, while (b) and (d) are images at corresponding magnifications of the night-time deposits.

Figure7. Images showing diatom association with calcareous deposits after 2 (a) and 7 (b) days of exposure, respectively, in the diurnal cycle.